Neurobiology of Disease 130 (2019) 104482

Contents lists available at ScienceDirect

Neurobiology of Disease

journal homepage: www.elsevier.com/locate/ynbdi

The loss of β adrenergic receptor mediated release potentiation in a mouse model of fragile X syndrome

Nuria García-Font[a,b,d], Ricardo Martín[a,b,d], Magdalena Torres[a,d], María Jesus Oset-Gasque[c,d], José Sánchez-Prieto[a,b,d,*]

[a] Departamento de Bioquímica, Facultad de Veterinaria, Universidad Complutense, 28040 Madrid, Spain
[b] Instituto Universitario de Investigación en Neuroquímica (IUIN), Universidad Complutense, 28040 Madrid, Spain
[c] Departamento de Bioquímica, Facultad de Farmacia, Universidad Complutense, 28040 Madrid, Spain
[d] Instituto de Investigación Sanitaria del Hospital Clínico San Carlos, 28040 Madrid, Spain

ARTICLE INFO

Keywords:
β adrenergic receptors
Glutamate release
cAMP
Cerebrocortical nerve terminals
Fmr1 KO mice
Fragile X syndrome
Phosphodiesterase 2
Docked synaptic vesicles
Ready releasable pool

ABSTRACT

In fragile X syndrome, the absence of Fragile X Mental Retardation Protein (FMRP) is known to alter postsynaptic function, although alterations in presynaptic function also occur. We found that the potentiation of glutamate release induced by the β adrenergic receptor (βAR) agonist isoproterenol is absent in cerebrocortical nerve terminals (synaptosomes) from mice lacking FMRP (*Fmr1* KO), despite the normal cAMP generation. The glutamate release induced by moderate stimulation of synaptosomes with 5 mM KCl was not potentiated in Fmr1 KO synaptosomes by isoproterenol, nor by stimulating the receptor associated signaling pathway with the adenylyl cyclase activator forskolin or with the Epac activator 8-pCPT. Hence, the impairment in the pathway potentiating release is distal to βARs. Electron microscopy shows that *Fmr1* KO cortical synapses have more docked vesicles than WT synapses, consequently occluding the isoproterenol response through which more SVs approach the active zone (AZ) of the plasma membrane. Weak stimulation of synaptosomes with the Ca^{2+} ionophore ionomycin recovered the release potentiation driven by forskolin and 8-pCPT but not with isoproterenol, revealing an impairment in the efficiency of receptor generated cAMP to activate the release potentiation pathway. Indeed, inhibiting cyclic nucleotide phosphodiesterase PDE2A with BAY 60–7550 reestablished isoproterenol mediated potentiation in *Fmr1* KO synaptosomes. Thus, the lack of β-AR mediated potentiation of glutamate release appears to be the consequence of an impaired capability of the receptor to mobilize SVs to the AZ and because of a decreased efficiency of cAMP to activate the signaling pathway that enhances neurotransmitter release.

1. Introduction

Fragile X syndrome (FXS) is the most common inherited intellectual disability and it is associated with multiple behavioral alterations, including cognitive deficits, hyperactivity, anxiety and deficits in social behavior (Hagerman et al., 2009 and MacLeod et al., 2010). In FXS, the *Fmr1* gene that encodes the fragile mental retardation protein (FMRP) is silenced. FMRP modulates gene expression through changes in the stability and transport of its mRNA targets (Kao et al., 2010; Zalfa et al., 2007) and acting as a suppressor of mRNA translation (Bassell and Warren, 2008) although in some cases FMRP activates translation (Liu et al., 2018; Bechara et al., 2009; Greenblatt and Spradling, 2018). In the absence of FMRP the expression of many postsynaptic proteins is altered as well as postsynaptic long-term forms of plasticity (Huber et al., 2002). FMRP is also found in axons and presynaptic nerve terminals (Akins et al., 2012; Christie et al., 2009) and mRNA targets encoding for presynaptic proteins were identified (Darnell et al., 2001; Darnell et al., 2011). Proteomic studies of mice lacking FMRP revealed a presynaptic phenotype (Klemmer et al., 2011) in which the expression of many presynaptic proteins is altered including those involved in

Abbreviations: FMRP, fragile mental retardation protein; cAMP, cyclic adenosine monophosphate; βAR, β adrenergic receptor; DAG, diacylglycerol; PKA, cAMP-dependent protein kinase; Epac, exchange protein directly activated by cAMP; 8-pCPT, 8-(4-chlorophenylthio)-2′-*O*-methyladenosine 3′,5′-cyclic monophosphate monosodium hydrate; AZ, active zone; SV, synaptic vesicle; AP, action potential; RRP, Readily releasable pool; TTx, Tetrodotoxin; FXS, Fragile X syndrome; NDS, normal donkey serum; PDE, phosphodiesterase; HBM, HEPES buffered medium; BSA, bovine serum albumin; IBMX, 3-isobutyl-1-methylxanthine; PB, phosphate buffer; TBS, Tris phosphate buffer; PSD, postsynaptic density; AZ, active zone; GC, guanylyl cyclase.

* Corresponding author at: Departamento de Bioquímica, Facultad de Veterinaria, Universidad Complutense, 28040 Madrid, Spain.
E-mail address: jsprieto@vet.ucm.es (J. Sánchez-Prieto).

https://doi.org/10.1016/j.nbd.2019.104482
Received 11 April 2019; Received in revised form 17 May 2019; Accepted 22 May 2019
Available online 23 May 2019

active zone structure, vesicle recycling and neurotransmitter release (Christie et al., 2009; Liao et al., 2008; Klemmer et al.., 2011; Tang et al., 2015).

The loss of FMRP enlarges the action potential (AP) and the ensuing influx of Ca^{2+} (Deng et al., 2013), contributes to increase the size of the readily releasable pool (RRP) of synaptic vesicles (SVs) (Thanawala and Regehr, 2013). The increase in the number of docked vesicles found in *Fmr1* KO neurons (Deng et al., 2011) could be responsible for the enhanced neurotransmitter release at synapses lacking FMRP (Deng et al., 2013), particularly as the number of docked vesicles strongly correlates with the size of the RRP of SVs (Rosenmund and Stevens, 1996; Schikorski and Stevens, 2001). In addition to Ca^{2+}, the increase in diacylglycerol (DAG) levels due to the loss of DAG kinase (Tabet et al., 2016) in *Fmr1* KO cells can also contribute to enlarge the size of the RRP through the activation of Munc13 proteins. Munc13 activity is regulated by the DAG (Betz et al., 2001), and by the Ca^{2+}-calmodulin (CaM) (Dimova et al., 2006; Dimova et al., 2009) and Ca^{2+}-phospholipid binding domains (Shin et al., 2010). Munc13 promotes the open conformation of syntaxin and initiates SNARE complex formation, which mediates the tight membrane attachment of SVs and makes them competent for release (Augustin et al., 1999; Varoqueaux et al., 2002; Imig et al., 2014).

β adrenergic receptors (βARs) at presynaptic nerve terminals enhance neurotransmitter release through the G protein dependent generation of cAMP and the ensuing activation of the guanine nucleotide exchange protein directly activated by cAMP (Epac), driving Munc13–1 translocation and an increase in the number of docked SVs (Ferrero et al., 2013). However, it is unknown whether βAR mediated potentiation of glutamate release is impaired at *Fmr1* KO synapses, although the RRP is already enhanced at these synapses and, cAMP signaling cascade is altered. Previous studies have shown a decreased cAMP production in cells from fragile X patients and *Fmr1* KO mice (Berry-Kravis and Huttenlocker, 1992; Berry-Kravis and Sklena, 1993) that can be reverted by FMRP overexpression (Berry-Kravis and Ciurlionis, 1998). In addition, a form of cAMP-dependent LTP that is expressed presynapticaly is impared in *Fmr1* KO mice (Koga et al., 2015a). The mRNA of the cAMP and cGMP degrading enzyme phosphodiesterase 2A (PDE2A) is a prominent target of FMRP in the cerebral cortex (Maurin et al., 2018a). Thus, the PDE2A enzymatic activity is increased in the brain of *Fmr1* KO mice (Maurin et al., 2018b) explaining why PDE2A inhibition rescued some behavior deficits in these animals (Maurin et al., 2018b).

Here we found that the glutamate release at *Fmr1* KO cerebrocortical nerve terminals induced by moderate stimulation (5 mM KCl) is not potentiated by the βAR agonist isoproterenol, nor by the adenylyl cyclase activator forskolin or the Epac activator 8-pCPT, despite the normal βAR expression and cAMP generation. *Fmr1* KO synapses have more docked vesicles and as isoproterenol fails to enhance docking, the recruitment of more SVs for release appears to be impeded. Interestingly, weaker stimulation of synaptosomes with the Ca^{2+} ionophore ionomycin recovered the release potentiation driven by forskolin and 8-pCPT but not by isoproterenol, revealing an impaired efficiency of receptor generated cAMP to activate the release potentiation pathway. Indeed, inhibiting cyclic nucleotide phosphodiesterase PDE2A with BAY 60–7550 reestablished isoproterenol mediated potentiation in *Fmr1* KO synaptosomes. As such, the lack of βAR mediated potentiation of glutamate release is the consequence of the impaired receptor capability to mobilize SVs to the active zone (AZ) of the plasma membrane, together with an impairment in the efficiency of cAMP to activate the signaling pathway that enhances neurotransmitter release.

2. Materials and methods

2.1. Synaptosomal preparation

In these experiments, all animal handling was performed in accordance with European Commission guidelines (2010/63/UE) and was approved by the Animal Research Committee at the Complutense University. Synaptosomes from the cerebral cortex of 3 adult C57BL/6 mice (2–4 months old) were purified on discontinuous Percoll gradients (GE Healthcare, Uppsala, Sweden) as described previously (Millan et al., 2002). Briefly, the tissue was homogenized in medium containing 0.32 M sucrose [pH 7.4], the homogenate was centrifuged for 2 min at 2000 x*g* and 4 °C, and the supernatant, S_1, was then centrifuged again for 12 min at 9500 x*g*. From the pellets obtained, P_2, the loosely compacted white layer containing the majority of the synaptosomes was gently resuspended in 0.32 M sucrose [pH 7.4] and an aliquot of this synaptosome suspension (2 ml) was placed onto a 3 ml Percoll discontinuous gradient containing: 0.32 M sucrose; 1 mM EDTA; 0.25 mM DL-dithiothreitol; and 3, 10 or 23% Percoll [pH 7.4]. After centrifugation at 25,000 x*g* for 10 min at 4 °C, the synaptosomes were recovered from between the 10% and the 23% Percoll bands, and they were diluted in a final volume of 30 ml HEPES buffered medium (HBM: 140 mM NaCl, 5 mM KCl, 5 mM $NaHCO_3$, 1.2 mM NaH_2PO_4, 1 mM $MgCl_2$, 10 mM glucose and 10 mM HEPES [pH 7.4]). Following further centrifugation at 22,000 x*g* for 10 min, the synaptosome pellet was resuspended in 0.5–1 ml of HBM medium and the protein content was determined by the Biuret method. Finally, 0.75 mg of the synaptosomal suspension was diluted in 2 ml HBM and centrifuged at 10,000 x*g* for 10 min. The supernatant was discarded and the pellet containing the synaptosomes was stored on ice. Under these conditions, the synaptosomes remain fully viable for at least 4–5 h.

2.2. Glutamate release

Glutamate release was assayed by on-line fluorimetry, as described previously (Millan et al., 2002). Synaptosomal pellets were resuspended in HBM (0.67 mg/ml) and preincubated at 37 °C for 1 h in the presence of 16 μM bovine serum albumin (BSA) to bind any free fatty acids released by the synaptosomes during the preincubation (Herrero et al., 1991). Adenosine deaminase (1.25 U/mg: Roche Diagnostics, Barcelona, Spain) was added for 15 min, and a 1 ml aliquot of the synaptosomes was transferred to a stirred cuvette containing 1 mM $NADP^+$, 50 U glutamate dehydrogenase (Sigma, St. Louis, MO, USA) and 1.33 mM $CaCl_2$, measuring the fluorescence of NADPH in a Perkin Elmer LS-50 luminescence spectrometer at excitation and emission wavelengths of 340 and 460 nm, respectively. The data were obtained at 0.8 s intervals and the fluorescence traces were calibrated by the addition of 2 nmols of glutamate at the end of each assay. The traces plotted are the mean of all the individual traces corresponding to a given condition. Smoothing protocols were applied to reduce the noise using OriginPro 8 and the Savitzky-Golay method.

The Ca^{2+}-dependent release was calculated by subtracting the release obtained during a 5-min period of depolarization at 200 nM free [Ca^{2+}] from the release at 1.33 mM $CaCl_2$. Glutamate release was also induced with the Ca^{2+} ionophore ionomycin, which was added in the presence of the Na^+-channel blocker tetrodotoxin (1 μM: Abcam, Cambridge, UK), to prevent the firing of action potentials and therefore, the AP driven opening of voltage dependent Ca^{2+} channels. The ionomycin-induced release was calculated by subtracting the release observed during a 8-min period in the absence of ionomycin (basal) from that observed in its presence. The concentration of ionomycin (Calbiochem, Darmstadt, Germany) was fixed in each experiment (0.5–1.0 μM) in order to achieve a release of 0.5–0.7 nmols glu/mg protein. Finally, the spontaneous glutamate release was determined in the absence of any stimulation but in the presence of the Na^+-channel blocker tetrodotoxin. In these experiments the βAR agonist isoproterenol (100 μM) (Sigma-Aldrich, St. Louis, MO, USA), the adenylyl cyclase activator forskolin (15 μM) and the phosphodiesterases inhibitor IBMX (1 mM) (Calbiochem, Damstard, Germany), the Epac activator 8-pCPT (50 μM) (Biolog, Life Science Institute, Bremen, Germany), the PDE2A inhibitor BAY60–7550 (0.5-10 μM) and the PDE4

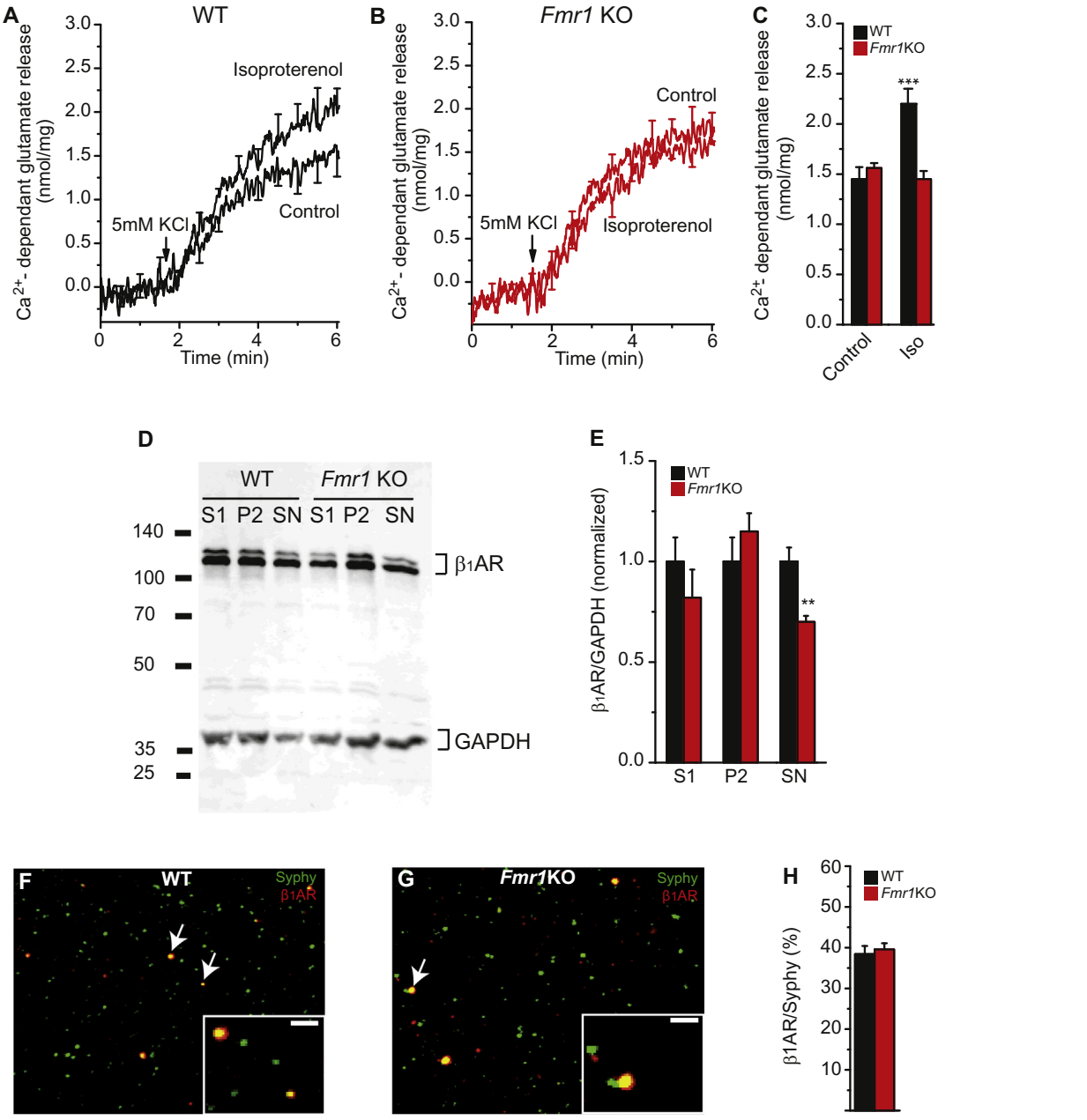

Fig. 1. Isoproterenol fails to potentiate KCl-induced release in *Fmr1* KO synaptosomes.
A, B, Mean traces from wild type (A) and *Fmr1* KO (B) cerebrocortical synaptosomes showing the release of glutamate evoked by 5 mM KCl in the presence and absence (control) of isoproterenol (100 μM) added 1 min prior to KCl. C, Diagram summarizing the glutamate release under these conditions. D, E, Western blot analysis of β1AR amount in S1, P2 and synaptosomes obtained from WT and *Fmr1* KO mice. β1AR dimers are readily observed. Data were normalized to WT values. Immunofluorescence of WT (F) and *Fmr1* KO (G) synaptosomes fixed onto poly-L-lysine-coated coverslips and stained with antibodies against: β1AR/synaptophysin. H, Quantification of the β1AR expression in synaptophysin-containing WT and *Fmr1* KO nerve terminals. The inset shows the region indicated by arrows at a higher magnification. The results are the mean ± S.E.M.: NS $P > .05$, ** $P < .005$, *** $P < .001$, compared to the corresponding control. ANOVA with Bonferroni's test in release experiments and unpaired Student's *t*-test in immunofluorescence and western blot experiments were used. Scale bar 5 μm.

inhibitor Rolipram (2-50 μM) (Abcam, Cambridge, UK) and the NO donor DEANO (20-μM) (Cayman Chemicals, Ann Harbor, MI, USA) were used.

2.3. Western blotting

S1, P2 and synaptosomes proteins (see synaptosomal preparation) (4 μg of protein per lane) were diluted in Laemmli loading buffer with β-mercaptoethanol (5% *v*/v), resolved in SDS-PAGE (8% acrylamide, Bio-Rad), and analyzed by Western blotting according to standard procedures. The proteins were transferred to PVDF membranes (Hybond ECL: GE Healthcare Life Sciences, Madrid, Spain). After several washes the membranes were probed with primary antibodies: polyclonal rabbit anti-β1AR (1:200, Santa Cruz Biotechnology, Paso Robles, CA, USA) and monoclonal mouse anti-GAPDH (1:10000, Sigma, St Louis, MO, USA). After several washes, the membranes were incubated with the corresponding IRD-labeled secondary antibodies: goat anti-rabbit and goat anti-mouse coupled to Odyssey IRDye 800 or Odyssey IRDye 680 (Rockland Immunochemicals, Gilbertsville, PA, USA). The membranes were scanned in an Odyssey Infrared imaging system, and the immunolabeling of proteins was compared by densitometry and quantified using Odyssey 2.0 software. The data were

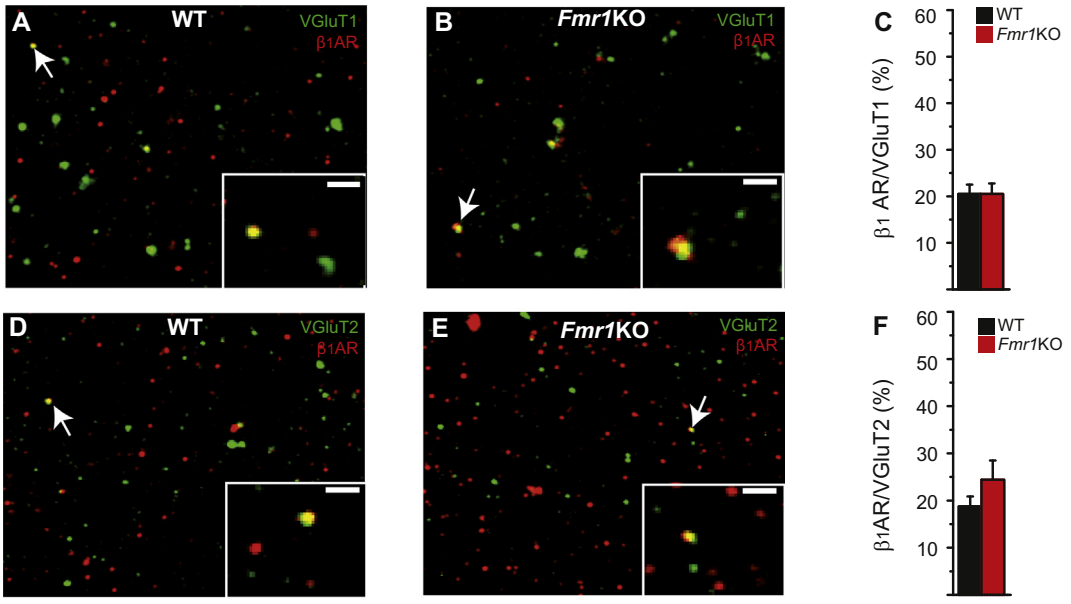

Fig. 2. Expression of βARs with vGlut1 and vGlut2 in cerebrocortical synaptosomes.
Immunofluorescence of WT (A,D) and *Fmr1* KO (B,E) cerebrocortical synaptosomes fixed onto poly-L-lysine-coated coverslips and stained with antibodies against: β1AR/vGlut1 (A,B) and β1AR/vGlut2 (D,E). C,F, Quantification of the β1AR expression in vGluT1- and vGluT2- containing WT and *Fmr1* KO nerve terminals. The inset shows the region indicated by arrows at a higher magnification. The results are the mean ± S.E.M.: NS $P > .05$, compared to the corresponding WT data using unpaired Student's t-test. Scale bar 5 µm.

normalized to the GAPDH signal to account for loading differences.

2.4. The cytosolic free Ca^{2+}

The cytosolic free Ca^{2+} concentration, $[Ca^{2+}]_c$, concentration was measured with fura-2. Synaptosomes were resuspended (1.5 mg/ml) in HBM with 16 µM BSA in the presence of 1.3 mM $CaCl_2$ and 5 µM fura-2-acetoxymethyl ester (fura 2-AM, Molecular Probes, Eugene, OR, USA), and they were incubated at 37 °C for 25 min. After fura-2 loading, the synaptosomes were pelleted and resuspended in 1.1 ml fresh HBM medium without BSA. A 1 ml aliquot was transferred to a stirred cuvette and 1.3 mM $CaCl_2$ was added. The fluorescence was monitored at 340 and 510 nm. Data points were taken at 0.3 s intervals and the $[Ca^{2+}]_c$, was calculated using the equations described previously by Grynkiewicz et al., 1985.

2.5. cAMP levels

The accumulation of cAMP was determined using a cAMP dynamic 2 kit (Cisbio, Bioassays, Bagnols sur-Cèze, France) as described previously (Ferrero et al., 2016). Synaptosomes were incubated for 30 min at 37 °C (0.67 mg/ml) in HBM containing 16 uM BSA and adenosine deaminase (1.25 U/mg protein). After 15 min, 1 mM of a cAMP phosphodiesterase inhibitor, 3-isobutyl-1-methylxanthine (IBMX: Calbiochem, Damstard, Germany) was added and the synaptosomes were then incubated with the β-AR agonist (100 µM isoproterenol) for 10 min. The synaptosomes were collected by centrifugation for 1 min at 4 °C and 16,000 xg, and they were resuspended (0.34 mg/ml) in HBM containing 16 µM BSA and 1 mM IBMX. The synaptosomes were transferred to a 96-well assay plate and the following components were added, diluted in lysis buffer (50 mM HEPES, 0.8 M potassium fluoride, 0.2% [*w*/*v*] BSA, 1% [*v*/v] Triton X-100 [pH 7.0]): the europium cryptate-labeled anti cAMP antibody and the d2-labeled cAMP analog. After incubation for 1 h at room temperature (RT), the europium cryptate fluorescence and TR-FRET signals were measured 50 ms after excitation at 337 nm on a FluoStar Omega microplate reader (BMG Lab Technologies, Offenburg, Germany) at 620 and 665 nm, respectively. The specific FRET (ΔF) signal was calculated using the following equation: ΔF % = 100 × (Rpos x Rneg)/(Rneg), where Rpos is the fluorescence ratio (665/620 nm) calculated in the wells incubated with both donor- and acceptor-labeled antibodies, and Rneg is the same ratio for the negative control incubated with only the donor fluorophore-labeled antibody. The FRET signal (ΔF%), which is inversely proportional to the concentration of cAMP in the synaptosomes, was then transformed to the accumulated cAMP value using a calibration curve prepared using the same plate.

2.6. Immunocytochemistry

Immunocytochemistry was performed using the following antibodies: affinity-purified rabbit polyclonal antiserum against β1AR (1:200) (Santa Cruz Biotechnology, Paso Robles, CA, USA); goat anti-β1AR antibody (1:200) (Sigma, St Louis, MO, USA); mouse monoclonal antibody against synaptophysin 1 (1:500); mouse monoclonal Munc13–1 antibody (1:500); rabbit anti Munc13–2 antibody (1:500), mouse monoclonal anti vGlut1 antibody (1:500) and mouse anti vGlut2 antibody (1:500) all from (Synaptic Systems, Gottingen, Germany). The procedure was as described previously (Ferrero et al., 2016). As a control for immunochemistry, the primary antibodies were omitted from the staining procedure, whereupon no immunoreactivity resembling that obtained with the specific antibodies was detected.

Synaptosomes (0.67 mg/ml) were added to medium containing 0.32 M sucrose [pH 7.4] at 37 °C, allowed to attach to poly-L-lysine coated coverslips for 1 h and then fixed for 4 min with 4% paraformaldehyde in 0.1 M phosphate buffer (PB, pH 7.4) at RT. Following several washes with 0.1 M PB [pH 7.4], the synaptosomes were pre-incubated for 1 h in 10% normal donkey serum (NDS, Jackson ImmunoResearch, West Grove, PA,USA) diluted in 50 mM Tris buffer [pH 7.4] containing 0.9% NaCl (TBS) and 0.2% Triton X-100. Subsequently, they were incubated overnight at 4 °C with the appropriate primary antiserum against β1ARs (1:200) and synaptophysin (1:500), diluted in TBS with 1% NDS and 0.2% Triton X-100. After washing in TBS, the synaptosomes were incubated with secondary antibodies diluted (1:200) in TBS for 2 h: Alexa fluor 488 Donkey anti-mouse IgG; Alexa fluor 488 Donkey anti-goat IgG and Alexa fluor 594 Donkey anti-rabbit IgG (Molecular Probes, Eugene, OR, USA). After

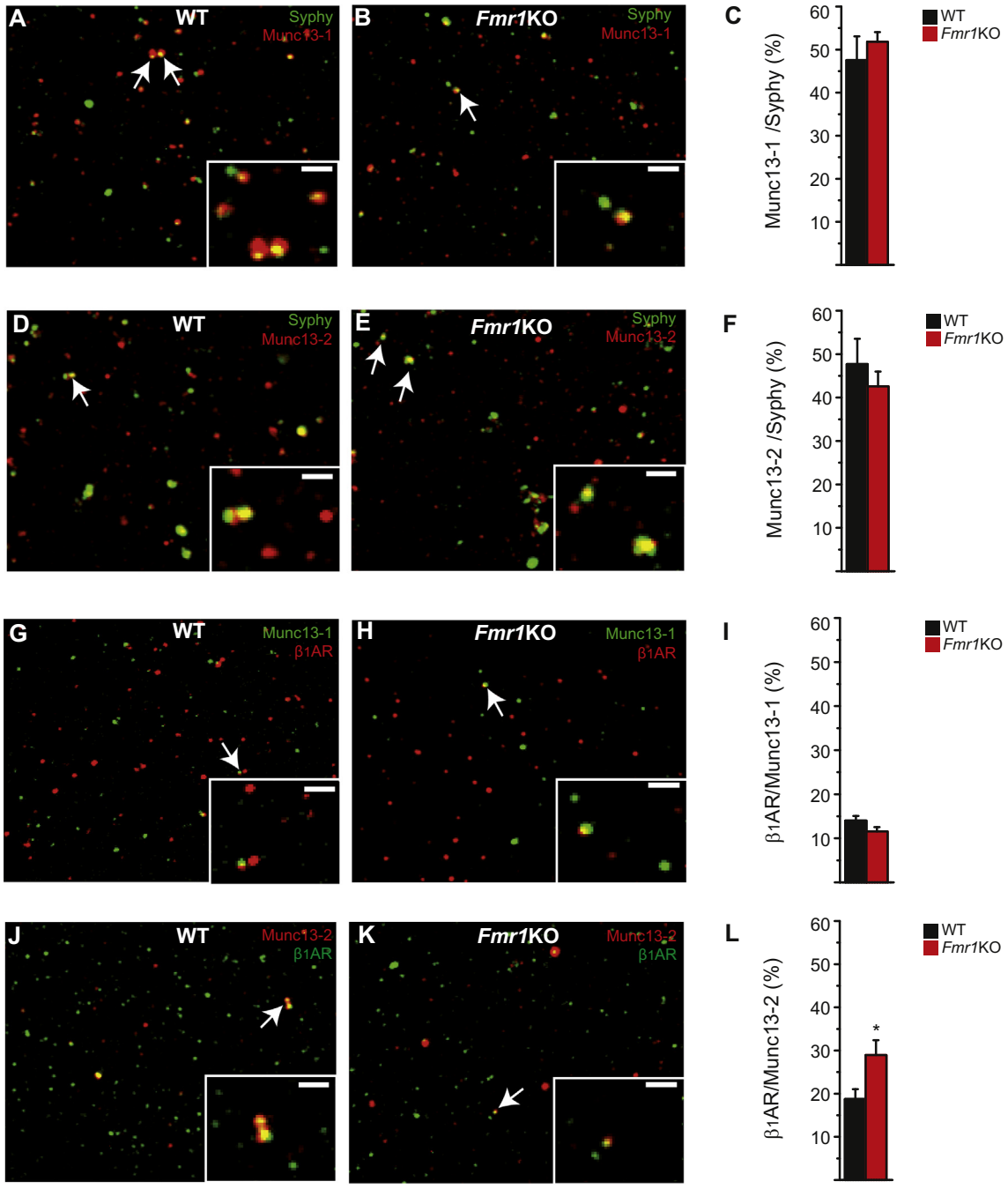

Fig. 3. Co-expression of βARs with Munc13–1 and Munc13–2 in cerebrocortical synaptosomes.
Immunofluorescence of WT (A,D,G,J) and *Fmr1* KO (B,E,H,K) cerebrocortical synaptosomes fixed onto poly-L-lysine-coated coverslips and stained with antibodies against: Munc13–1/synaptophysin (A,B); Munc13–2/synaptophysin (D,E); β1AR/Munc13–1 (G,H); β1-AR/Munc13–2 (J,K). Quantification of the data (C,F,I,L). The inset shows the region indicated by arrows at a higher magnification. The results are presented as the mean ± S.E.M.: * $P < .05$ compared to the corresponding WT data using an unpaired Student's t-test. Scale bar 5 µm.

several washes in TBS, the coverslips were mounted with Prolong Antifade Kit (Molecular Probes, Eugene, OR, USA) and the synaptosomes were viewed on a Nikon Diaphot microscope equipped with a 100× objective, a mercury lamp light source and Nikon fluorescein-rhodamine filter sets.

For quantification, all the images were acquired using identical settings and neutral density transmittance filters. Background subtraction was performed by applying a rolling ball algorithm (10 pixel radius), and the brightness and contrast settings were adjusted according to the negative control values using Image J 1.39f (http://rsb.info.nih.gov/ij). The number of stained particles larger than 0.5 µm was quantified automatically from the binary image masks, discarding aggregates. Co-localization analysis was performed automatically by measuring the area of coincidence of particles quantified in each pair of images within the same field.

2.7. Analysis of synaptic vesicle distribution at the active zone by electron microscopy

Coronal vibratome slices (325 µm thick: Leica VT 1200S vibratome) were obtained in ice-cold Ringer's solution (119 mM NaCl, 2.5 mM KCl, 1.3 mM $MgSO_4$, 2.5 mM $CaCl_2$, 26 mM $NaHCO_3$, 1 mM NaH_2PO_4,

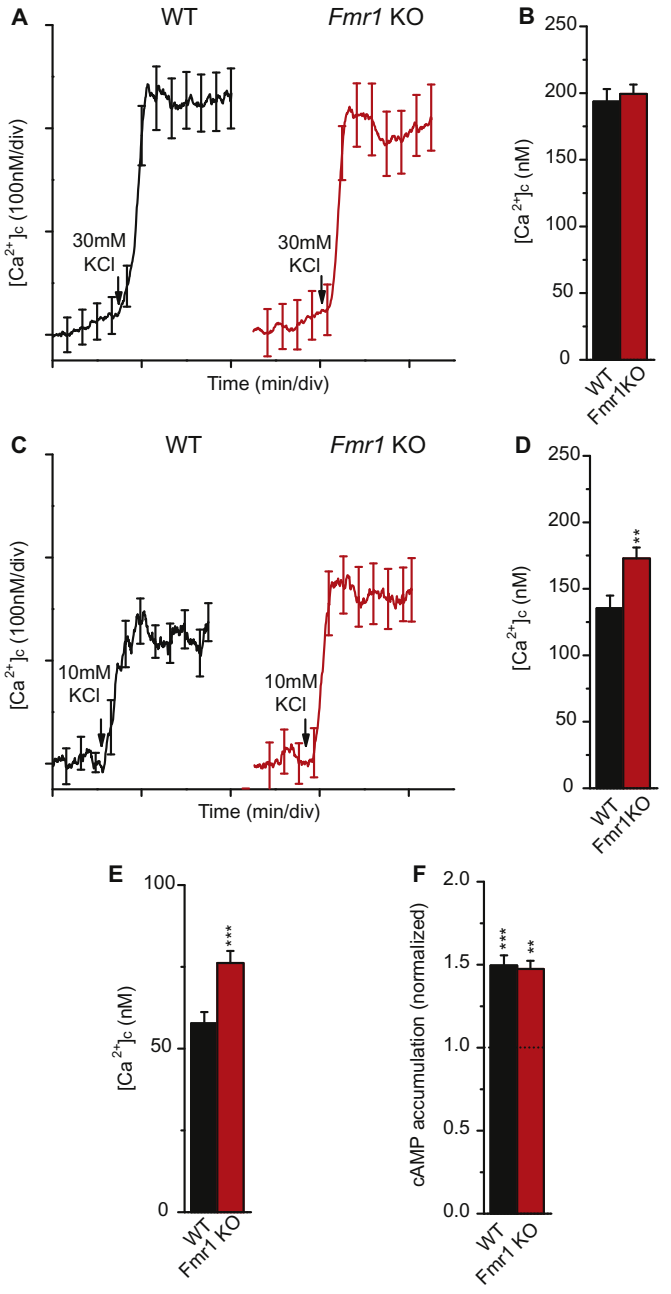

Fig. 4. Enhanced Ca^{2+} influx but normal cAMP generation in *Fmr1* KO synaptosomes.
(A,C), The Ca^{2+} influx was estimated as the increase in cytoplasmic free Ca^{2+} concentration, $[Ca^{2+}]_c$ induced by 30 and 10 mM KCl depolarization in fura-2 loaded WT and *Fmr1* KO synaptosomes. (B,D), Bar diagrams showing the increase in Ca^{2+} in the different conditions. (E), Increase in $[Ca^{2+}]_c$ induced by Ca^{2+} addition prior to depolarization in WT and *Fmr1* KO synaptosomes. (F), Isoproterenol increases the cAMP levels to a similar extent in WT and *Fmr1* KO nerve terminals. Isoproterenol (100 μM) was added 5 min after IBMX (see Materials and Methods). The results are presented as the mean ± S.E.M.: ** $P < .01$, *** $P < .001$ compared to the corresponding WT data using an unpaired Student's t-test.

10 mM glucose) and kept in a holding chamber containing Ringer's solution for at least 1 h. After transferring the slices to a superfusing chamber for recording, the Ringer's solution was supplemented with 50 μM picrotoxin (to block $GABA_A$ receptors) and it was equilibrated in 95% O_2/5% CO_2. The flow rate was 1 ml/min and the temperature was maintained at 25 °C using a temperature controller (TC-324C Warner-Instruments), treating the slices for 10 min with isoproterenol (100 μM) in some cases. Immediately afterwards, the slices were fixed for 45 min at 37 °C by immersion in 3.5% glutaraldehyde in PB and they were then left in the glutaraldehyde solution for 30 min at RT before storing them for 20 h at 4 °C. The slices were then rinsed six times with large volumes of 0.1 M PB and the cerebral cortices were dissected out, post-fixing them in 1% OsO_4–1.5% $K_3Fe(CN)_6$ for 1 h at RT. After dehydrating through a graded series of ethanol (30, 50, 70, 80, 90, 95 and 100%), the samples were embedded using the SPURR embedding kit (TAAB, Aldermaston, UK). Ultrathin ultramicrotome sections (70–80 nm thick: Leica EM UC6 Leica Microsystems, Wetzlar, Germany) were routinely stained with uranyl acetate and lead citrate, and images were obtained on a Jeol 1010 transmission electron microscope (Jeol, Tokyo, Japan). Randomly chosen areas from layers II/III of somatosensory cortex were then photographed at 80,000× magnification and only asymmetric synapses with clearly identifiable electron-dense postsynaptic densities (PSDs) were analyzed, measuring them with ImageJ software. The relative percentage of SVs per AZ was calculated in 10 nm bins at the AZ of the inner layer membrane and the total number of SVs per synaptic terminal was also determined. The data were analyzed blind to the genotype and treatment.

2.8. Statistical analysis

The data were analyzed using GraphPad. InStat (2. 05a) software, employing ANOVA with Bonferroni's test or the unpaired two-tailed Student's *t*-test. The data are represented as the mean ± S.E.M.: $*p < .05$, $**p < .01$, $***p < .001$. Differences were considered statistically significant when $p < .05$ with a confidence limit of 95%.

3. Results

3.1. Isoproterenol fails to enhance KCl evoked release in Fmr1 KO synaptosomes

The depolarization of synaptosomes with a low concentration of KCl induces submaximal release of glutamate, allowing this release to be further potentiated by Gs coupled βARs that target the release machinery (Ferrero et al., 2013). In wild type (WT) cerebrocortical synaptosomes, KCl (5 mM) induced a release, measured in nmols of glutamate/mg protein of (1.45 ± 0.12, $n = 16$) was potentiated by the βAR agonist isoproterenol (100 μM: 2.20 ± 0.15, n = 16, $P < .001$, Fig. 1A,C), consistent with the receptor capability to generate cAMP and its subsequent effect on the release machinery (Ferrero et al., 2013). By contrast, isoproterenol failed to enhance release in synaptosomes that lack FMRP, isolated from *Fmr1* KO mice (1.45 ± 0.08 and 1.56 ± 0.05 in the presence and absence of isoproterenol, $n = 9$, $P > .05$: Fig. 1B,C).

The expression of βARs was determined by western blotting. No change was found in *Fmr1* KO S1 (82.0 ± 14%, $n = 4$, $P = .3559$) and P2 (115 ± 9%, n = 4, $P = .3667$) fractions compared to WT. However, β1ARs expression in *Fmr1* KO synaptosomes was reduced to (70 ± 3.0%, n = 4, $P = .0076$, Fig. 1D,E) of WT. To assess that a decreased expression of β1ARs occurs in *Fmr1* KO synaptosomes we performed immunofluorescence experiments in the whole population of nerve terminals using antibodies against β1ARs and the SVs protein synaptophysin. No change was found between WT (38.4 ± 2.0% of cerebrocortical synaptosomes double labeled with β1AR/synaptophysin, $n = 23$, fields: Fig. 1F,H) and *Fmr1* KO synaptosomes (39.6 ± 1.5% double labeled with β1ARs/synaptophysin ($n = 25$ fields, $P = .64$: Fig. 1G,H). We also studied β1ARs expression by immunofluorescence in the subpopulation of glutamatergic nerve terminals with antibodies against the vesicular glutamate transporters vGlut1 and vGlut2. No change was found between WT (20.5 ± 2.0%, $n = 15$ and 18.8 ± 2.1%, $n = 9$, Fig. 2A,C,D,F) and *Fmr1* KO (20.5 ± 2.3%, $n = 13$, $P = .99$ and 24.4 ± 4.1, $n = 11$, $P = .26$, of

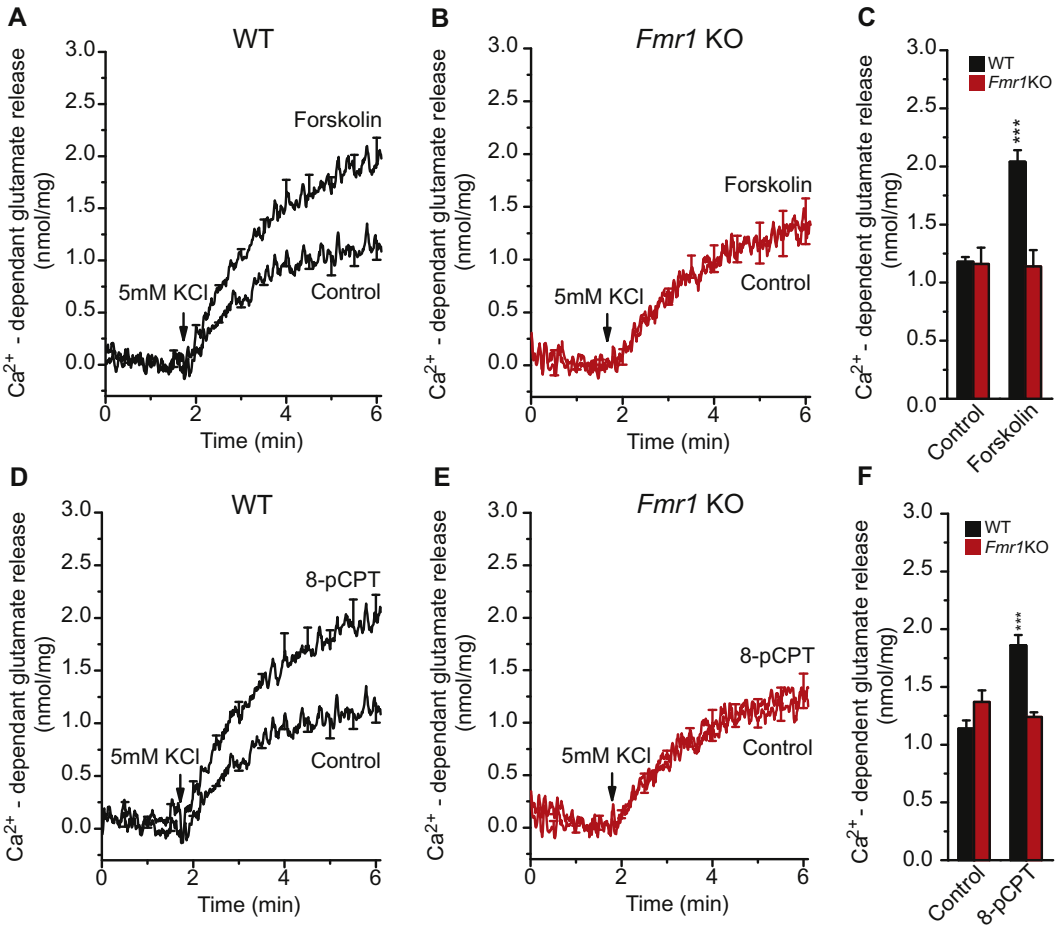

Fig. 5. Activation of the βAR-associated signaling pathway at the level of the adenylyl cyclase (forskolin) or Epac proteins (8-pCPT) also fails to enhance KCl-evoked release.

Mean traces from wild type (A,D) and *Fmr1* KO (B,E) cerebrocortical synaptosomes showing the release of glutamate evoked by 5 mM KCl in the absence (control) and in the presence of forskolin (15 μM: A,B) or 8-pCPT (50 μM: D,E), added 1 min prior to KCl. Diagrams summarizing release in the presence of forskolin (C) and 8-pCPT (F). The results are presented as the mean ± S.E.M.: *** $P < .001$. compared to the corresponding control. ANOVA with Bonferroni's test.

synaptosomes double labeled with βAR/vGlut1, and βAR/vGlut2, respectively, Fig. 2B,C,E,F). Then, immunofluorescence experiments do not support that a change in the expression of β1ARs in *Fmr1* KO glutamatergic nerve terminals is responsible for the lack of isoproterenol dependent potentiation of glutamate release.

Munc13 proteins play a central role in the potentiation of neurotransmitter release (Rhee et al., 2002; Rosenmund et al., 2002). We found that the expression of Munc13–1 and Munc13–2 was similar in the whole population of WT (47.6 ± 5.5%, n = 9 and 47.7 ± 5.9%, n = 9, Fig. 3A,C,D,F) and *Fmr1* KO synaptosomes (51.8 ± 2.3%, n = 9, $P = .49$ and 42.6 ± 3.4%, n = 9, $P = .4702$, of synaptosomes double labeled for Munc13–1/synaptophysin and Munc13–2/synaptophysin, respectively, Fig. 3B,C,E,F). Although, the expression of Munc13–1 and Munc13–2 proteins is not altered in the whole population of nerve terminals, more βARs are expressed in Munc13–2-containing nerve terminals of *Fmr*1 KO (11.5 ± 1.0%, $n = 26$, $P = .12$ and 29.0 ± 3.5%, $n = 14$, $P = .0189$ Fig. 3H,I,K,L) compared to WT animals (14.0 ± 1.1%, n = 15 and 18.8 ± 2.3%, n = 14, of synaptosomes double labeled for βAR/Munc13–1 and βAR/Munc13–2, respectively, Fig. 3G,I,J,L). As Munc13–2 is also involved in the potentiation of neurotransmitter release (Rosenmund et al., 2002; Martin et al., 2018) it is unlikely that the enrichment of βAR in the Munc13–2-containing subpopulation of *Fmr1* KO nerve terminals is responsible for the lack of βAR mediated potentiation.

Ca^{2+} homeostasis is altered in fragile X syndrome (Deng et al., 2013; Ferron et al., 2014; Castagnola et al., 2018). We measured the depolarization induce Ca^{2+} influx in fura-2 loaded synaptosomes. The 10 mM KCl induced responses in synaptosomes are sensitive to the Na^+ channel tetrodotoxin indicative of the generation of action potentials, but not those by 30 mM KCl responses (Godino et al., 2007). We found that Ca^{2+} influx with 30 mM KCl was similar in WT (193.6 ± 9.4 nM, $n = 29$) and *Fmr1* KO synaptosomes (199.3 ± 7.1 nM, $n = 20$, $P = .63$, Fig. 4A,B). However, Ca^{2+} influx induced by 10 mM KCl was larger in *Fmr1* KO (172.8 ± 8.2 nM, $n = 12$, $P = .009$) than in WT (135.4 ± 9.6 nM, $n = 8$, Fig. 4C,D) compatible with prolonged action potentials of *Fmr1* KO synapses (Deng et al., 2013). The $[Ca^{2+}]_c$ levels prior to depolarization were also higher in *Fmr1* KO (76.2 ± 3.7 nM, $n = 21$, $P = .0008$) than in WT synaptosomes (57.7 ± 3.4 nM, $n = 18$, Fig. 4E). Then, Ca^{2+} homeostasis is deregulated in *Fmr1* KO cerebrocortical synaptosomes.

βARs activate adenylyl cyclase to generate cAMP, which activates downstream signaling to potentiate spontaneous release (Ferrero et al., 2013). However, the failure of isoproterenol to potentiate release is not due to receptor inability to generate cAMP, as the increase in cAMP induced by isoproterenol in WT synaptosomes (149.6 ± 6.0%, $n = 10$) was similar to that in *Fmr1* KO synaptosomes (147.4 ± 5.0%, n = 8, $P = .99$: Fig. 4F) consistent with immunofluorescence experiments showing no change in receptor expression.

The adenylyl cyclase activator forskolin (15 μM) enhanced glutamate release in WT synaptosomes (2.04 ± 0.10 and 1.18 ± 0.04 in the presence and absence of forskolin, n = 10, $P < .001$: Fig. 5A,C) but not in *Fmr1* KO synaptosomes (1.14 ± 0.14 and 1.16 ± 0.14 in the

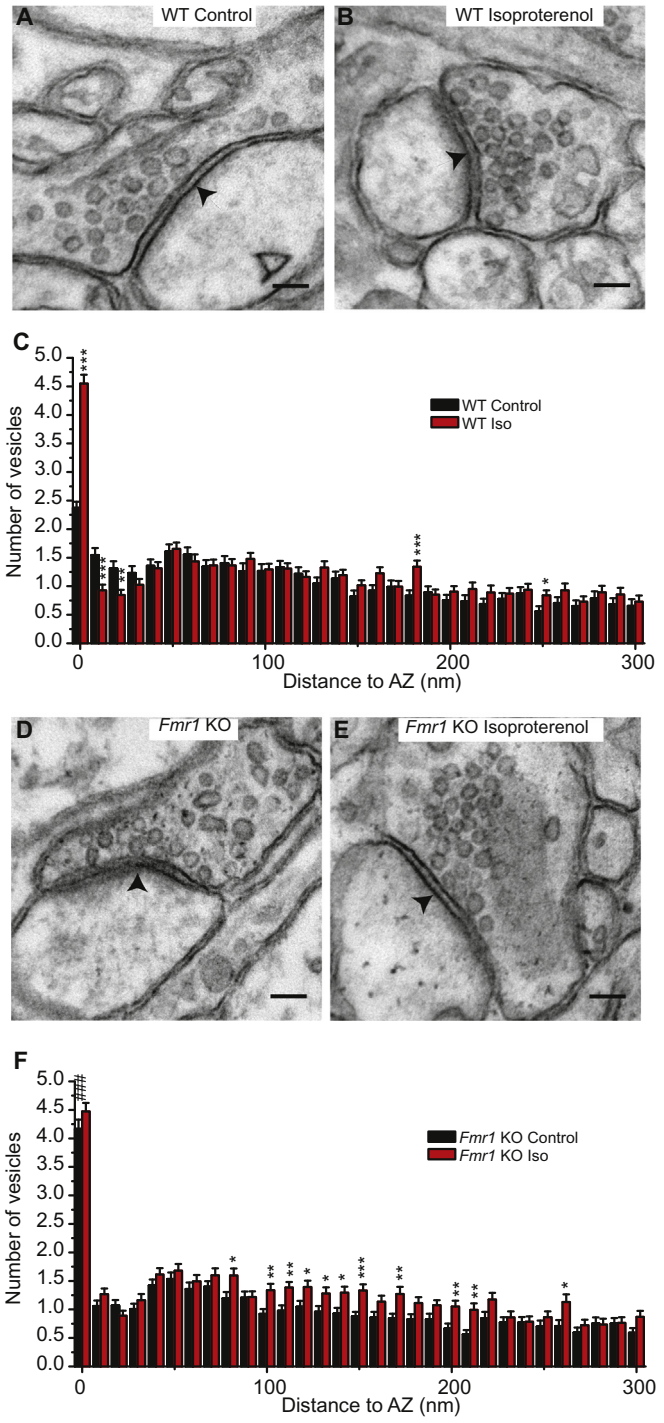

Fig. 6. Cerebrocortical synapses lacking FMRP have more docked synaptic vesicles than WT synapses and isoproterenol fails to enhance docking.
The treatment of cerebrocortical slices with isoproterenol (100 μM, 10 min) affects the distribution of SVs closer than 10 nm from the AZ of the plasma membrane in both WT (A,B,C) and *Fmr1* KO synapses (D,E,F). C, F, Quantification of the changes in SV distribution induced by isoproterenol at WT (C) and Fmr1 KO (F) synapses. The data are the mean ± S.E.M: * P < .05, ** P < .01, *** P < .001 compared to the corresponding control slices (untreated). ### P < .001 compared to the control data between WT and *Fmr1* KO. ANOVA with Bonferroni's test. Scale bar in A, B, D and E 100 nm.

presence and absence of forskolin, n = 8, $P > .05$: Fig. 5B,C). Thus, the impairment of βAR mediated potentiation occurs downstream of cAMP.

Isoproterenol-induced potentiation of glutamate release requires the exchange proteins directly activated by cAMP, Epac (Ferrero et al., 2013) which have emerged as alternative cAMP targets in neurotransmitter release (Huang and Hsu, 2006; Gekel and Neher, 2008; Ferrero et al., 2013; Fernandes et al., 2015). Thus, the Epac activator 8-pCPT (50 μM) enhanced glutamate release in WT synaptosomes (from 1.14 ± 0.07, $n = 5$, to 1.86 ± 0.09, $n = 7$, $P < .001$: Fig. 5D,F), although it failed to enhance such release in *Fmr1* KO synaptosomes (1.37 ± 0.10 and 1.24 ± 0.05, n = 5, $P > .05$: Fig. 5E,F).

3.2. *Fmr1 KO synapses have more docked SVs*

The finding that stimulating the signaling cascade triggered by isoproterenol at different levels failed to potentiate glutamate release suggests that the impairment may occur distal to receptor signaling, affecting the release machinery. The βAR mediated potentiation of glutamate release involves an increase in the number of docked SVs (Ferrero et al., 2013), while the distribution of SVs at the AZ of *Fmr1* KO hippocampal synapses is altered (Deng et al., 2011). We found that *Fmr1* KO cerebrocortical synapses have more docked vesicles (4.17 ± 0.16, $n = 131$ synapses: Fig. 6D,F) than WT synapses (2.38 ± 0.11, $n = 112$ synapses $P < .001$: Fig. 6A,C). As βAR mediated potentiation of release is associated with an increase in the docked SVs, it is likely that the failure of βARs to potentiate release reflects the failure of this receptor to augment SV docking at *Fmr1* KO synapses. Indeed, isoproterenol failed to augment the SVs docked at *Fmr1* KO synapses (4.47 ± 0.15, $n = 135$ synapses and 4.17 ± 0.16, n = 131 synapses, in the presence and absence of isoproterenol, $P > .05$: Fig. 6E,F), while isoproterenol did increase the docked SVs at WT synapses (from 2.38 ± 0.11, n = 112 synapses to 4.55 ± 0.16, $n = 124$ synapses, P < .001: Fig. 6B,C). Then, the capability of βARs to increase docking of SVs is occluded at *Fmr1* KO cerebrocortical synapses.

3.3. *Forskolin and 8-pCPT but not isoproterenol enhance ionomycin-induced glutamate release at Fmr1 KO synapses*

The number of docked SVs is strongly correlated to the size of the RRP of vesicles (Rosenmund and Stevens, 1996; Schikorski and Stevens, 2001), which represents the vesicles ready to fuse that define the release probability and synaptic strength. We measured the spontaneous release of glutamate after blocking Na^+ channels with TTX in order to prevent APs. The spontaneous release of glutamate from WT synaptosomes was increased by isoproterenol from 1.54 ± 0.07 nmols of glutamate/mg protein (n = 5) to 2.05 ± 0.06 ($n = 6$, $P < .001$: Fig. 7A,C). By contrast, in *Fmr1* KO synaptosomes the stronger spontaneous release (1.94 ± 0.06, n = 5, $P < .01$) was not affected by isoproterenol (2.01 ± 0.08, $n = 4$, $P > .05$: Fig. 7B,C). Then, the spontaneous release reflects the number of docked vesicles and its potentiation by isoproterenol is occluded in *Fmr1* KO synaptosomes.

Spontaneous glutamate release results from spontaneous fusion of one vesicle that occurs at resting concentrations of cytosolic Ca^{2+} or after the stochastic opening of one Ca^{2+} channel (Kaeser and Regehr, 2014). Given that evoked release is more relevant physiologically, we induced Ca^{2+} dependent release with the Ca^{2+} ionophore, ionomycin, which inserts into the membrane and delivers Ca^{2+} to the interior of the cell, thereby inducing glutamate release. One advantage of ionomycin is that we can adjust the concentration of ionomycin to release only a small amount of glutamate, which might represent a fraction of the RRP of SVs. In WT synaptosomes, ionomycin-induced release (0.47 ± 0.03 nmols of glutamate/mg protein, n = 12) was enhanced by isoproterenol (0.84 ± 0.05, $n = 17$, $P < .001$: Fig. 8A,C), yet isoproterenol failed to enhance glutamate release from *Fmr1* KO synapses (0.47 ± 0.03, $n = 16$ and 0.49 ± 0.03, $n = 13$, in the presence and absence of isoproterenol, $P > .05$: Fig. 8B,C). Thus, isoproterenol also fails to potentiate glutamate release, even when a weak stimulation is used. By contrast, the adenylyl cyclase activator forskolin enhanced the ionomycin-induced release in *Fmr1* KO synaptosomes (1.16 ± 0.09, $n = 6$ and 0.58 ± 0.03, $n = 2$, in the presence and absence of

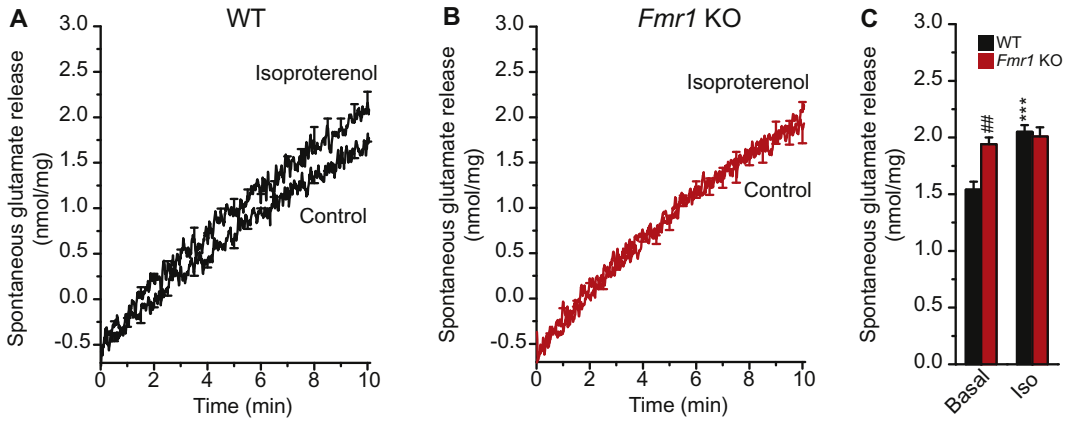

Fig. 7. The lack of FMRP increases the spontaneous release of glutamate and occludes isoproterenol induced potentiation.
The spontaneous release of glutamate was measured in the absence of any stimulation and in the presence of the Na^+ channel blocker tetrodotoxin (1 μM) added 2–3 min prior to measuring spontaneous release. A,B, Isoproterenol (100 μM) increases the spontaneous release from WT (A) but not in *Fmr1* KO (B) synaptosomes. C, Quantification of the changes in spontaneous release under these conditions: *** P < .001 compared to the corresponding control data (untreated) ## P < .01 comparing the basal data between WT and *Fmr1* KO slices. ANOVA with Bonferroni's test.

forskolin, $P < .05$: Fig. 8E,F), as well as in WT synaptosomes (1.30 ± 0.11 nmols, n = 6 and 0.61 ± 0.05, $n = 4$, in the presence and absence of forskolin, $P < .01$ Fig. 8D,F). The activation of the βAR signaling cascade at the level of Epac proteins with 8-pCPT, also potentiated the ionomycin-induced release in *Fmr1* KO synaptosomes (1.07 ± 0.07, $n = 11$ and 0.50 ± 0.03, n = 4, in the presence and absence of 8-pCPT, $P < .001$: Fig. 8H,I) to a similar extent as in WT synaptosomes (1.14 ± 0.06, $n = 7$ and 0.58 ± 0.04, n = 4, in the presence and absence of 8-pCPT, P < .001: Fig. 8G,I). Thus, weak stimulation of synaptosomes recovered the potentiation of glutamate release in *Fmr1* KO synaptosomes, yet only when the βAR dependent signaling cascade was activated downstream of the receptor.

3.4. Inhibiting phosphodiesterase PDE2A restores the isoproterenol induced potentiation of release

The failure of isoproterenol but not of forskolin or 8-pCPT to enhance ionomycin-induced release is not due to a failure in receptor signaling, as a similar amount of cAMP is found in *Fmr1* KO and WT synaptosomes in the presence of isoproterenol. However, the lower efficiency of cAMP to activate downstream targets could be related to changes in cAMP metabolism due to enhanced phosphodiesterase activity (Maurin et al., 2018b). We found that the inhibition of phosphodiesterase activity with the pan-inhibitor IBMX restored the potentiation of isoproterenol-induced release in *Fmr1* KO synaptosomes (0.84 ± 0.03 nmols of glutamate/mg protein, $n = 15$, P < .001, Fig. 9B,G). A similar result was obtained with the specific PDE2A inhibitor BAY 60–7550 (2 μM) (0.90 ± 0.05, n = 6, P < .01, Fig. 9C,G) but not with the specific PDE4 inhibitor rolipram (50 μM) (0.68 ± 0.04, n = 4, $P > .05$, Fig. 9D,G). Control release of *Fmr1* KO synaptosomes in the absence of isoproterenol was (0.49 ± 0.03, n = 13, Fig. 9A,G). Then, PDE2A activity seems to be responsible for the low efficiency of cAMP to activate the signaling pathway leading to glutamate release potentiation. cGMP binds to PDE2A and induces a conformational change that increases several times its activity to metabolize cAMP (Zhang et al., 2015). We tested whether increasing PDE2A activity abolish isoproterenol-induced potentiation of release in WT synaptosomes. A way to increase cGMP levels is with a nitric oxide (NO) donor through guanylate cyclase stimulation. We found that the NO donor DEANO abolishes the isoproterenol-induced potentiation of release in WT synaptosomes (0.96 ± 0.05, $n = 12$, P < .001 and 0.50 ± 0.03, $n = 9$, P > .05, in the absence and presence of DEANO, Fig. 9E,F,H). Then, the lack of βAR mediated potentiation of glutamate release is a consequence of the impaired capability of these receptors to mobilize SVs to the AZ of the plasma membrane and to the weaker efficiency of cAMP to activate the signals that potentiate neurotransmitter release.

4. Discussion

The data presented here show that βAR activation fails to potentiate glutamate release at *Fmr1* KO synapses because they have more docked vesicles and consequently, βAR activation fails to induce further docking. Weak stimulation of synaptosomes with ionomycin reveals the lower efficiency of cAMP to activate the potentiation pathway, as the adenylyl cyclase activator forskolin and the Epac activator 8-pCPT but not the βAR agonist isoproterenol potentiate glutamate release. Indeed, inhibiting cyclic nucleotide phosphodiesterase PDE2A with BAY 60–7550 reestablishes the isoproterenol mediated potentiation in *Fmr1* KO synaptosomes. Thus, the lack of βAR mediated potentiation of glutamate release reflects the impaired capacity of the receptor to mobilize SVs to the AZ and the decreased efficiency of cAMP to activate the signaling that enhances neurotransmitter release (See Graphical Abstract).

β-ARs potentiate glutamate release via Gs protein dependent generation of cAMP and the subsequent activation of Epac and PLC which drives Munc13–1 translocation and increases docked SVs (Ferrero et al., 2013). Presynaptic receptors coupled to cAMP generation also increase the SV size (Steuer Costa et al., 2017). The number of docked SVs correlates strongly with the size of the RRP (Rosenmund and Stevens, 1996; Schikorski and Stevens, 2001), which represents the vesicles that are ready to fuse with the plasma membrane. Moderate stimulation (KCl 5 mM) of synaptosomes prevents β-AR mediated potentiation of release likely due to the depletion of the RRP. The RRP represents only a fraction of the recycling pool of SVs (Rizzoli and Betz, 2005) and β-ARs fail to induce further SV docking at *Fmr1* KO synapses. The occlusion of the isoproterenol-induced increase in docking could result from the enhanced docking that basally exists at *Fmr1* KO synapses (Deng et al., 2011). Munc13 proteins play an essential role in SV docking through the formation of the Munc13-Rim1-Rab3 (Dulubova et al., 2005) and the SNARE complex. (Ma et al., 2011). An excess of SV docking could result from increased Munc13 activity driven by the enhanced DAG (Tabet et al., 2016) and Ca^{2+} levels, which are also deregulated at *Fmr1* KO synapses (Ferron et al., 2014; Castagnola et al., 2018, and Fig. 4C,D,E). FMRP directly interacts with voltage gated Ca^{2+} channels altering Ca^{2+} homeostasis through reduction of Ca^{2+} channels degradation and increasing channel density at nerve terminals (Ferron et al., 2014; Castagnola et al., 2018). The lack of FMRP also

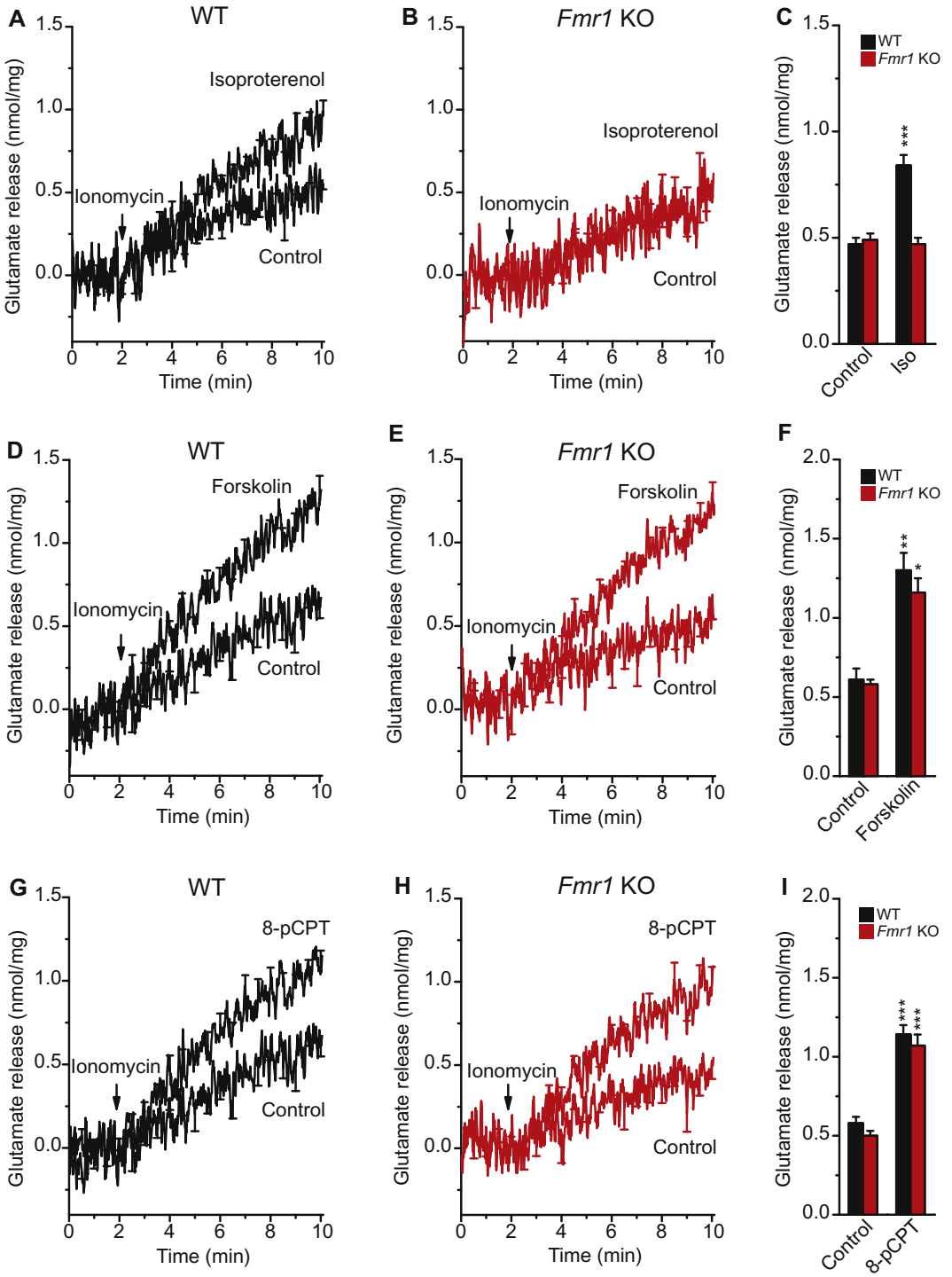

Fig. 8. Activating the βAR signaling pathway at the level of the adenylyl cyclase (forskolin) or Epac proteins (8pCPT), yet not with the agonist isoproterenol, enhances ionomycin induced release.

Mean traces from wild type (A,D,G) and *Fmr1* KO (B,E,H) cerebrocortical synaptosomes showing the release of glutamate induced by ionomycin in the presence or absence (control) of isoproterenol (100 μM: A,B), forskolin (15 μM: D,E) and 8-pCPT (50 μM: G,H), added 1 min prior ionomycin. C, F, I, Diagrams summarizing the glutamate release with isoproterenol (C), forskolin (F) and 8-pCPT (I). The results are presented as the mean ± S.E.M.: * P < .05, ** P < .01, *** P < .001, compared to the corresponding control. ANOVA with Bonferroni's test.

indirectly increases Ca^{2+} influx by action potential broadening due to decreased function of Ca^{2+} activated K^+ channels (Deng et al., 2013) Therefore, understanding the factors that contribute to the enhanced docking at *Fmr1* KO synapses is essential to propose pharmacological strategies to restore the distribution of SVs and presynaptic potentiation by βARs.

Further evidence that a deficit in SV availability underlies the impaired release is the recovery of β-ARs-mediated potentiation when the stimulus intensity is reduced with the Ca^{2+} ionophore ionomycin to induce a control release to 0.5–0.7 nmols. This weak stimulation with ionomycin, however, uncovered a decrease in the efficiency of cAMP signaling as release potentiation is restored when the βAR signaling

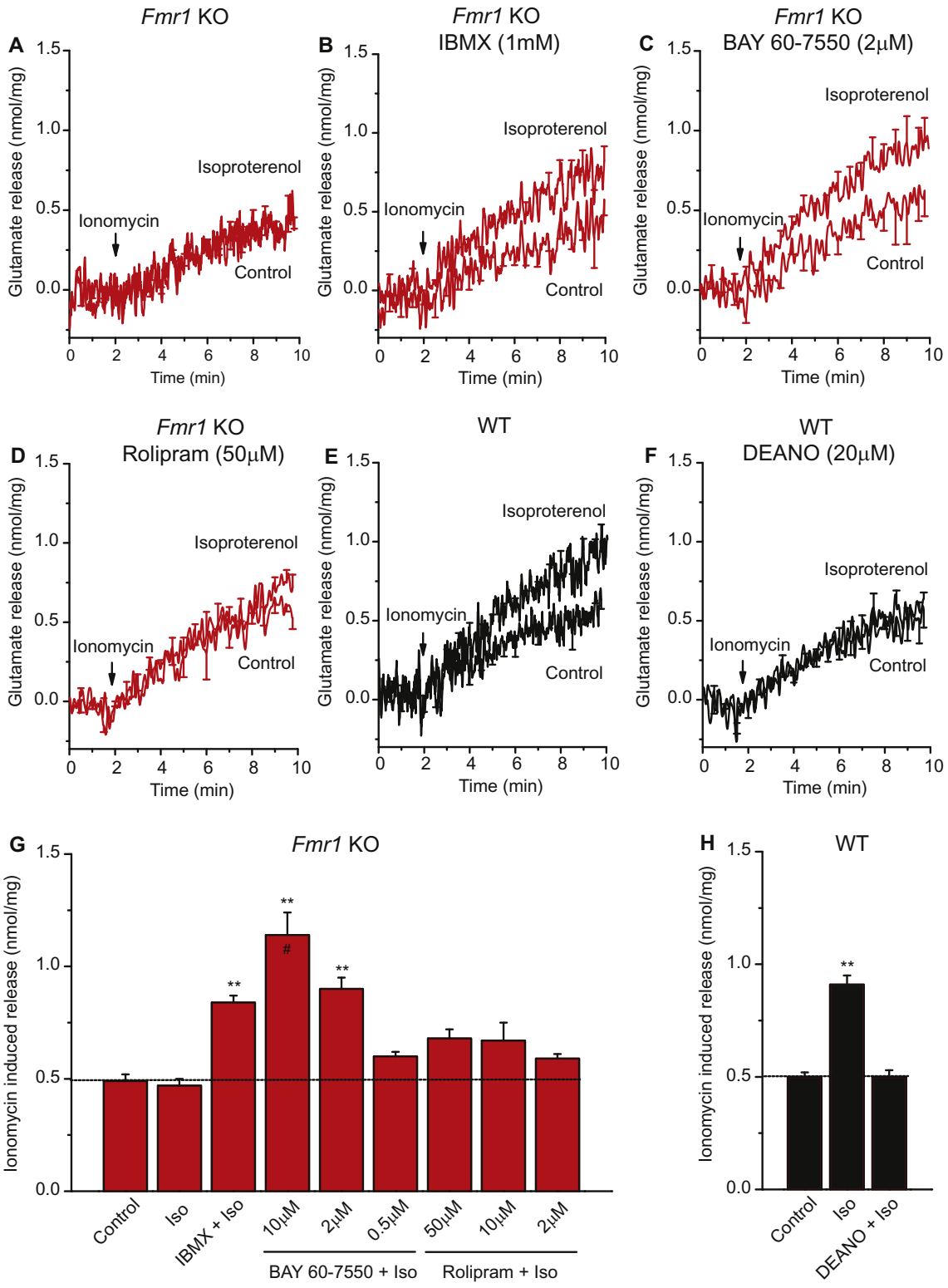

Fig. 9. Inhibiting phosphodiesterase PDE2A with BAY 607550 fully rescues isoproterenol potentiation of the ionomycin-induced release.
Mean traces from *Fmr1* KO (A,B,C,D) and WT (E,F) cerebrocortical synaptosomes showing the release of glutamate induced by ionomycin in the presence of isoproterenol (100 μM) added 1 min prior to ionomycin. The broad spectrum phosphodiesterase inhibitor IBMX (1 mM, B); the PDE2 inhibitor BAY 607550 (2 μM, C) and the PDE4 inhibitor Rolipram (50 μM, D) were added 15 min prior to performing the release assay. The NO donor DEANO (20 μM, F) was added 3 min prior to ionomycin. G,H, Diagrams summarizing the glutamate release data in *Fmr1* KO (G) and WT (H) synaptosomes. The results are means ± S.E.M.: ** $P < .01$, compared to the respective control and # $P < .05$ compared to the WT control using. ANOVA with Bonferroni's test.

pathways is activated downstream of the receptor with forskolin or 8-pCPT, yet not with the receptor agonist isoproterenol. As the generation of cAMP by the receptor is not impaired in *Fmr1* KO synapses, one possibility is that cAMP is degraded more rapidly in *Fmr1* KO than in WT cells (Maurin et al., 2018b). It is important to note that any potential difference in cAMP degradation will be masked in the cAMP assay, as the pan-phosphodiesterase inhibitor IBMX is included. Remarkably, the potentiation of ionomycin-induced release by isoproterenol is restored with the pan-PDE inhibitor IBMX and with specific PDE2A inhibitor BAY 60–7550, but not with the specific inhibitor of PDE4 rolipram. Then, a decreased efficiency of cAMP to potentiate release occurs at *Fmr1* KO synapses as a consequence of altered PDE2A activity.

PDE2A is strongly expressed at glutamatergic pyramidal cells in the cortex (Stephenson et al., 2012) and this protein is localized presynaptically in the active zone associated with docked vesicles (Boyken et al., 2013). The PDE2A mRNA is a prominent target of FMRP in the cerebral cortex (Maurin et al., 2018a) and the PDE2A protein is upregulated at *Fmr1 KO* cortical synapses (Tang et al., 2015) as well as its enzymatic activity (Maurin et al., 2018b). Then, this PDE2A de-regulation can contribute to a less efficient cAMP signaling and account for the loss of βAR mediated potentiation of glutamate release at *Fmr1* KO synaptosomes. Thus, the specific inhibitor of PDE2A BAY 60–7550 fully rescues isoproterenol-induced potentiation of glutamate release. Inhibiting PDE2A activity restores other presynaptic functions of FMRP such as the control of axonal growth (Maurin et al., 2018b). PDE2A is also postsynaptic and its pharmacological inhibition rescue the maturity of dendritic spines, and the exaggerated hippocampal mGluR-dependent LTP (Maurin et al., 2018b). Another link between PDE activity and FXS is provided by the finding that IBMX, but not by PDE4 inhibitor Rolipram rescue sensory processing in Drosophila Fragile X syndrome mutants (Androschuck et al., 2018).

The NO donor DEANO triggers guanylate cyclase activity and cGMP, which enhances PDE2A activity. In WT synaptosomes DEANO abolished isoproterenol-induced potentiation of glutamate release. Thus, cGMP can be a potential modulator of the efficiency of cAMP signaling. The cGMP and cAMP degrading phosphodiesterase PDE2A is up-regulated in *Fmr1* KO synapses (Tang et al., 2015) and therefore low levels of both nucleotides are expected in *Fmr1* KO cells making unlikely the stimulating effect of cGMP on PDE2A. NO triggers GC activation and increases cGMP which inhibits glutamate release (Sistiaga et al., 1997) and depresses the SVs RRP (Stanton et al., 2003). Then, an increase in cGMP levels would cause depression of synaptic transmission by its direct negative effect on the RRP and through an indirect effect increasing PDE2A activity and decreasing the efficiency of cAMP signaling.

To date many studies have focused on the postsynaptic functions of FMRP although this protein also plays a role in presynaptic compartments. Presynaptic FMRP regulates glutamate release onto neocortical inhibitory neurons (Patel et al., 2013), protein synthesis-dependent long-term plasticity (Till et al., 2011), and action potential with dependence on large-conductance calcium-activated potassium channels (Myrick et al., 2015). Presynaptic Long Term Potentiation (LTP) in the anterior cingulate cortex (ACC) is absent in *Fmr1* KO mice (Koga et al., 2015a). This form of presynaptic plasticity requires Ca^{2+}-stimulated adenylyl cyclase and the activation of cAMP/PKA dependent pathways (Koga et al., 2015b). However, it is not known whether pre-LTP in the ACC requires the synaptic potentiation produced by βARs, despite the important role of the ACC in learning, memory and emotional processing (Frankland et al., 2004), and that mice lacking FMRP suffer from learning deficits and anxiety (Guo et al., 2012). Therefore, it will be important to explore whether pre-LTP in the ACC requires the contribution of βARs and whether the recovery of βAR mediated potentiation of synaptic transmission helps to restore brain functions altered in fragile X syndrome.

In conclusion, the data presented here show that the lack of βAR mediated potentiation of glutamate release is a consequence of the impaired capability of these receptors to mobilize SVs to the AZ of the plasma membrane and to the weaker efficiency of cAMP to activate the signals that potentiate neurotransmitter release.

Acknowledgements

This work was financed by grants to JS-P and MT from the Spanish 'MINECO' (BFU 2013-43163R and BFU-2017-83292R to JS-P), the 'Instituto de Salud Carlos III' (RD 16/0019/0009) and the 'Comunidad de Madrid' (CAM-I2M2 2011-BMD-2349 and Program MULTITARGET& VIEW-CM, B2017/BMD-3688). We also thank Marisa García and Miriam Gonzalez from the electron microscopy facility at the Universidad Complutense Madrid for their technical support, and María del Carmen Zamora for her excellent technical assistance. We thank Mark Sefton for editorial assistance.

Declaration of interest

None.

References

Myrick, L.K., Deng, P.-Y., Hashimoto, H., Oh, Y.M., Cho, Y., Poidevin, M.J., Suhl, J.A., Visootsak, J., Cavalli, V., Jin, P., et al., 2015. Proc. Natl. Acad. Sci. U. S. A. 112, 949–956. https://doi.org/10.1073/pnas.1423094112.

Rhee, J.S., Betz, A., Pyott, S., Reim, K., Varoqueaux, F., Augustin, I., Hesse, D., Sudhof, T.C., Takahashi, M., Rosenmund, C., et al., 2002. β phorbol ester- and diacylglycerol-induced augmentation of transmitter release is mediated by Munc13s and not by PKCs. Cell 108https://doi.org/10.1016/S0092-8674(01)00635-3. 121–33. 108:121-33.

Varoqueaux, F., Sigler, R., Rhee, J.S., Brose, N., Enk, C., Reim, K., Rosenmund, C., 2002. Total arrest of spontaneous and evoked synaptic transmission but normal synaptogenesis in the absence of Munc13-mediated vesicle priming. Proc. Natl. Acad. Sci. U. S. A. 99, 9037–9042. https://doi.org/10.1073/pnas.122623799.

Akins, M.R., Leblanc, H.F., Stackpole, E.E., Chyung, E., Fallon, J.R., 2012. Systematic mapping of fragile X granules in the mouse brain reveals a potential role for presynaptic FMRP in sensorimotor functions. J. Comp. Neurol. 520, 3687–3706. https://doi.org/10.1002/cne.23123.

Androschuck, A., He, R.X., Weber, S., Rosenfelt, C., Bolduc, F.V., 2018. Stress odorant sensory response dysfunction in drosophila fragile X syndrome mutants. Frontiers in Mol Neurosci. 11, 242. https://doi.org/10.3389/fnmol.2018.00242. (eCollection 2018).

Augustin, I., Rosenmund, C., Sudhof, T.C., Brose, N., 1999. Munc13-1 is essential for fusion competence of glutamatergic synaptic vesicles. Nature 400, 457–461. https://doi.org/10.1038/22768.

Bassell, G.J., Warren, S.T., 2008. Fragile X syndrome: loss of local mRNA regulation alters synaptic development and function. Neuron 60, 201–214. https://doi.org/10.1016/j.neuron.2008.10.004.

Bechara, E.G., Didiot, M.C., Melko, M., Davidovic, L., Bensaid, M., Martin, P., Castets, M., Pognomec, P., Khandjian, E.W., Moine, H., et al., 2009. A novel function for fragile X mental retardation protein in translation activation. PLoS Biol. 7, e16. https://doi.org/10.1371/journal.pbio.1000016.

Berry-Kravis, E., Ciurlionis, R., 1998. Overexpression of fragile X gene (FMR-1) transcripts increases cAMP production in neuronal cells. J. Neurosci. Res. 51, 41–48. https://doi.org/10.1002/(SICI)1097-4547(19980101)51:1<41::AID-JNR4>3.0.CO;2-L.

Berry-Kravis, E., Huttenlocker, P.R., 1992. Cyclic AMP metabolism in fragile X syndrome. Ann. Neurol. 31, 22–26. https://doi.org/10.1002/ana.410310105.

Berry-Kravis, E., Sklena, P., 1993. Demonstration of abnormal cyclic AMP production in platelets from patients with fragile X syndrome. Am. J. Med. Genet. 45, 81–87. https://doi.org/10.1002/ajmg.1320450120.

Betz, A., Thakur, P., Junge, H.J., Ashery, U., Rhee, J.S., Scheuss, V., Rosenmund, C., Rettig, J., Brose, N., 2001. Functional interaction of the active zone proteins Munc13-1 and RIM1 in synaptic vesicle priming. Neuron 30, 183–196. https://doi.org/10.1016/S0896-6273(01)00272-0.

Boyken, J., Grenborg, M., Riedel, D., Urlaub, H., Jahn, R., En Chua, J.J., 2013. Molecular profiling of synaptic vesicle docking sites reveals novel proteins but few differences between glutamatergic and GABAergic synapses. Neuron 78, 285–297. https://doi.org/10.1016/j.neuron.2013.02.027.

Castagnola, S., Delhaye, S., Folci, A., Paquet, A., Brau, F., Duprat, F., Jarjat, M., Grossi, M., Beal, M., Martin, S., et al., 2018. New insights into the role of Cav2 protein family in calcium influx deregulation in Fmr1 KO neurons. Frontiers in Mol. Neurosci. 11, 342. https://doi.org/10.3389/fnmol.2018.00342. (eCollection 2018).

Christie, S.B., Akins, M.R., Schwob, J.E., Fallon, J.R., 2009. The FXG: a presynaptic fragile X granule expressed in a subset of developing brain circuits. J. Neurosci. 29, 1514–1524. https://doi.org/10.1523/JNEUROSCI.3937-08.2009.

Darnell, J.C., Jensen, K.B., Jin, P., Brown, V., Warren, S.T., Darnell, R.B., 2001. Fragile X mental retardation protein targets G quartet mRNAs important for neuronal function.

Cell 107, 489–499. https://doi.org/10.1016/S0092-8674(01)00566-9.
Darnell, J.C., Van Driesche, S.J., Zhang, C., Hung, K.Y., Mele, A., Fraser, C.E., Stone, E.F., Chen, C., Fak, J.J., Chi, S.W., et al., 2011. FMRP stall ribosomes translocation of mRNAs linked to synaptic function and autism. Cell 146, 247–261. https://doi.org/10.1016/j.cell.2011.06.013.
Deng, P.-Y., Sojka, D., Klyachko, V.A., 2011. Abnormal presynaptic short term plasticity and information processing in a mouse model of Fragile X syndrome. J. Neurosci. 31, 10971–10982. https://doi.org/10.1523/JNEUROSCI.2021-11.2011.
Deng, P.-Y., Rotman, Z., Blundon, J.A., Cho, Y., Cui, J., Cavalli, V., Zakharenko, S.S., Klyachko, V.A., 2013. FMRP regulates neurotransmitter release and synaptic information transmission by modulating action potential duration via BK channels. Neuron 77, 696–711. https://doi.org/10.1016/j.neuron.2012.12.018.
Dimova, K., Kawabe, H., Betz, A., Brose, N., Jahn, O., 2006. Characterization of the Munc13-calmodulin interaction by photoaffinity labeling. Biochim. Biophys. Acta 1763, 1256–1265. https://doi.org/10.1016/j.bbamcr.2006.09.017.
Dimova, K., Kalkhof, S., Pottratz, I., Ihling, C., Rodriguez-Castaneda, F., Liepold, T., Griesinger, C., Brose, N., Sinz, A., Jahn, O., 2009. Structural insights into the calmodulin-Munc13 interaction obtained by cross-linking and mass spectrometry. Biochemistry 48, 5908–5921. https://doi.org/10.1021/bi900300r.
Dulubova, I., Lou, X., Lu, J., Huryeva, I., Alam, A., Schneggenburger, R., Sudhof, T.C., Rizo, J., 2005. A Munc13/RIM/Rab3 tripartite complex: from priming to plasticity? EMBO J. 24, 2839–2850. https://doi.org/10.1038/sj.emboj.7600753.
Fernandes, H.B., Riordan, S., Nomura, T., Remmers, C.L., Kraniotis, S., Marshall, J.J., Kukreja, L., Vassar, R., Contractor, A., 2015. Epac2 mediates cAMP-dependent potentiation of neurotransmission in the hippocampus. J. Neurosci. 35, 6544–6553. https://doi.org/10.1523/JNEUROSCI.0314-14.2015.
Ferrero, J.J., Alvarez, A.M., Ramírez-Franco, J., Godino, M.C., Bartolomé-Martín, D., Aguado, C., Torres, M., Luján, R., Ciruela, F., Sánchez-Prieto, J., 2013. beta-Adrenergic receptors activate EPAC, translocate Munc13-1 and enhance the Rab3A-Rim1alpha interaction to potentiate glutamate release at cerebrocortical nerve terminals. J. Biol. Chem. 288, 31370–31385. https://doi.org/10.1074/jbc.M113.463877.
Ferrero, J.J., Ramirez-Franco, J., Martin, R., Bartolome-Martin, D., Torres, M., Sánchez-Prieto, J., 2016. Cross-talk between metabotropic glutamate receptor 7 and beta-adrenergic receptor signaling at cerebrocortical nerve terminals. Neuropharmacology 101, 412–425. https://doi.org/10.1016/j.neuropharm.2015.07.025.
Ferron, L., Nieto-Rostro, M., Cassidy, J.S., Dolphin, A.C., 2014. Fragile X mental retardation protein controls synaptic vesicle exocytosis by modulatin N type calcium channels density. Nat. Commun. 5, 3628. https://doi.org/10.1038/ncomms4628.
Frankland, P.W., Bontempi, B., Talton, L.E., Kaczmarek, L., Silva, A.J., 2004. The involvement of the anterior cingulate cortex in remote contextual fear memory. Science 304, 881–883. https://doi.org/10.1126/science.1094804.
Gekel, I., Neher, E., 2008. Application of an Epac activator enhances neurotransmitter release at excitatory central synapses. J. Neurosci. 28, 7991–8002. https://doi.org/10.1523/JNEUROSCI.0268-08.2008.
Godino, M.C., Torres, M., Sanchez-Prieto, J., 2007. CB1 receptors diminish both Ca2+ influx and glutamate release through two different mechanisms active in distinct populations of cerebrocortical nerve terminals. J. Neurochem. 101, 1471–1482. https://doi.org/10.1111/j.1471-4159.2006.04422.x.
Greenblatt, E.J., Spradling, A.C., 2018. Fragile X mental retardation 1 gene enhances the translation of large autism-related proteins. Science 361, 709–712. https://doi.org/10.1126/science.aas9963.
Grynkiewicz, G., Poenie, M., Tsien, R.Y., 1985. A new generation of Ca2+ indicators with greatly improved fluorescence properties. J. Biol. Chem. 260, 3440–3450.
Guo, W., Murthy, A.C., Zhang, L., Johnson, E.B., Schaller, E.G., Allan, A.M., Zhao, X., 2012. Inhibition of GSK3improves hippocampus-dependent learning and rescues neurogenesis in a mouse model of fragile X syndrome. Hum. Mol. Genet. 21, 681–691. https://doi.org/10.1093/hmg/ddr501.
Hagerman, R.J., Berry-Kravis, E., Kaufmann, W.E., Ono, M.Y., Tartaglia, N., Lachiewicz, A., Kronk, R., Delahunty, C., Hessl, D., Visootsak, J., 2009. Advances in the treatment of fragile X syndrome. Pediatrics 123, 378–390. https://doi.org/10.1542/peds.2008-0317.
Herrero, I., Castro, E., Miras-Portugal, M.T., Sanchez-Prieto, J., 1991. Glutamate exocytosis evoked by 4-aminopyridine is inhibited by free fatty acids released from rat cerebrocortical synaptosomes. Neurosci. Lett. 126, 41–44. https://doi.org/10.1016/0028-3908(95)00067-G.
Huang, C.C., Hsu, K.S., 2006. Presynaptic mechanism underlying cAMP-induced synaptic potentiation in medial prefrontal cortex pyramidal neurons. Mol. Pharmacol. 69, 846–856. https://doi.org/10.1124/mol.105.018093.
Huber, K.M., Gallagher, S.M., Warren, S.T., Bear, M.F., 2002. Altered synaptic plasticity in a mouse model of fragile X mental retardation. Proc. Natl. Acad. Sci. U. S. A. 99, 7746–7750. https://doi.org/10.1073/pnas.122205699.
Imig, C., Min, S.W., Krinner, S., Arancillo, M., Rosenmund, C., Südhof, T.C., Rhee, J., Brose, N., Cooper, B.H., 2014. The morphological and molecular nature of synaptic vesicle priming at presynaptic active zones. Neuron 84, 416–431. https://doi.org/10.1016/j.neuron.2014.10.009.
Kaeser, P.S., Regehr, W.G., 2014. Molecular mechanisms for synchronous, asynchronous, and spontaneous neurotransmitter release. Annu. Rev. Physiol. 76, 333–363. https://doi.org/10.1146/annurev-physiol-021113-170338.
Kao, D.I., Aldridgeb, G.M., Weilerb, I.J., Greenough, W.T., 2010. Altered mRNA transport, docking, and protein translation in neurons lacking fragile X mental retardation protein. Proc. Natl. Acad. Sci. U. S. A. 107, 15601–15606. https://doi.org/10.1073/pnas.1010564107.
Klemmer, P., Meredith, R.M., Holmgren, C.D., Klychnikov, O.I., Stahl-Zeng, J., Loos, M., van der Schors, R.C., Wortel, J., de Wit, H., Spijker, S., 2011. Proteomics, ultrastructure, and physiology of hippocampal synapses in a fragile X syndrome mouse model reveal presynaptic phenotype. J. Biol. Chem. 286, 25495–25504. https://doi.org/10.1074/jbc.M110.210260.
Koga, K., Liu, M.-G., Qiu, S., Song, Q., O'Den, G., Chen, T., Zhuo, M., 2015a. Impaired presynaptic long-term potentiation in the anterior cingulate cortex of Fmr1 Knockout mice. J. Neurosci. 35, 2033–2043. https://doi.org/10.1523/JNEUROSCI.2644-14.2015.
Koga, K., Descalzi, G., Chen, T., Ko, H.G., Lu, J., Li, S., Son, J., Kim, T.H., Kwak, C., Huganir, R.L., et al., 2015b. Co-existence of two forms of LTP in ACC provides a synaptic mechanism for the interactions between anxiety and chronic pain. Neuron 85, 377–389. https://doi.org/10.1016/j.neuron.2015.05.016.
Liao, L., Park, S.K., Xu, T., Vanderklish, P., Yates III, J.R., 2008. Quantitative proteomic analysis of primary neurons reveals diverse changes in synaptic protein content in fmr1 knockout mice. Proc. Natl. Acad. Sci. U. S. A. 105, 15281–15286. https://doi.org/10.1073/pnas.0804678105.
Liu, B., Li, Y., Stackpole, E.S., Novak, A., Gao, Y., Zhao, Y., Zhao, X., Richter, J.D., 2018. Regulatory discrimination of mRNAs by FMRP controls mouse adult neural stem cell differentiation. Proc. Natl. Acad. Sci. U. S. A. 115, 11397–11405. https://doi.org/10.1073/pnas.1809588115.
Shin, O.H., Lu, J., Rhee, J.S., Tomchick, D.R., Pang, Z.P., Wojcik, S.M., Camacho-Perez, M., Brose, N., Machius, M., Rizo, J., et al., 2010. Munc13 C2B domain is an activity-dependent Ca2+ regulator of synaptic exocytosis. Nat. Struct. Mol. Biol. 17, 280–288. https://doi.org/10.1038/nsmb.1758.
Ma, C., Li, W., Xu, Y., Rizo, J., 2011. Munc13 mediates the transition from the closed syntaxin-Munc18 complex to the SNARE complex. Nat. Struct. Mol. Biol. 18, 542–549. https://doi.org/10.1038/nsmb.2047.
MacLeod, L.S., Kogan, C.S., Collin, C.A., Berry-Kravis, E., Messier, C., Gandhi, R., 2010. A comparative study of the performance of individuals with fragile X syndrome and Fmr1 knockout mice on Hebb-Williams mazes. Genes Brain Behaviour 9, 53–64. https://doi.org/10.1111/j.1601-183X.2009.00534.x.
Martin, R., Ferrero, J.J., Collado-Alsina, A., Aguado, C., Lujan, R., Torres, M., Sanchez-Prieto, J., 2018. Bidirectional modulation of glutamatergic synaptic transmission by metabotropic glutamate type 7 receptors at Schaffer collateral-CA1 hippocampal synapses. J. Physiol. 596, 921–940. https://doi.org/10.1113/JP275371.
Maurin, T., Lebrigand, K., Castagnola, S., Paquet, A., Jarjat, M., Popa, A., Grossi, M., Rage, F., Bardoni, B., 2018a. HITS-CLIP in various brain areas revelas new targets and new modalities of RNA binding by fragile X mental retardation protein. Nucleic Acids Res. 46, 6344–6355. https://doi.org/10.1093/nar/gky267.
Maurin, T., Melancia, F., Jarjat, M., Castro, L., Costa, L., Delhaye, S., Khayachi, A., Castagnola, S., Mota, E., Di Giorgio, A., et al., 2018b. Involvement of phosphodiesterase 2A activity in the pathophysiology of fragile X syndrome. Cereb. Cortex 2018. https://doi.org/10.1093/cercor/bhy192.
Millan, C., Lujan, R., Shigemoto, R., Sanchez-Prieto, J., 2002. The inhibition of glutamate release by metabotropic glutamate receptor 7 affects both $[Ca^{2+}]_c$ and cAMP: evidence for a strong reduction of Ca^{2+} entry in single nerve terminals. J. Biol. Chem. 277, 14092–14101. https://doi.org/10.1074/jbc.M109044200.
Patel, A.B., Hays, S.A., Bureau, I., Huber, K.M., Gibson, J.R., 2013. A target cell-specific role for presynaptic Fmr1 in regulating glutamate release onto neocortical fast-spiking inhibitory neurons. J. Neurosci. 33, 2593–2604. https://doi.org/10.1523/JNEUROSCI.2447-12.2013.
Rizzoli, S.O., Betz, W.J., 2005. Synaptic vesicle pools. Nat. Rev. Neurosci. 6, 57–69. https://doi.org/10.1038/nrn1583.
Rosenmund, C., Stevens, C.F., 1996. Definition of the readily releasable pool of vesicles at hippocampal synapses. Neuron 16, 1197–1207. https://doi.org/10.1016/S0896-6273(00)80146-4.
Rosenmund, C., Sigler, A., Augustin, I., Reim, K., Brose, N., Rhee, J.S., 2002. Differential control of vesicle priming and short term plasticity by Munc13 isoforms. Neuron 33, 411–424. https://doi.org/10.1016/S0896-6273(02)00568-8.
Schikorski, T., Stevens, C.F., 2001. Morphological correlates of functionally defined synaptic vesicle populations. Nat. Neurosci. 4, 391–395. https://doi.org/10.1038/86042.
Sistiaga, A., Miras-Portugal, M.T., Sanchez-Prieto, J., 1997. Modulation of glutamate reléase by a nitric oxyde/cyclic GMP-dependent pathway. Eur. J. Pharmacol. 321, 247–257. https://doi.org/10.1016/S0014-2999(96)00937-5.
Stanton, P.K., Winterer, J., Bailey, C.P., Kyozis, A., Raginov, I., Laube, G., Veh, R.W., Nguyen, C.Q., Muller, W., 2003. Long-term depression of presynaptic release from the readily releasable pool induced by NMDA receptor-dependent retrograde nitric oxide. J. Neurosci. 23, 5936–5944. https://doi.org/10.1523/JNEUROSCI.23-13-05936.
Stephenson, D.T., Coskran, T.M., Kelly, M.P., Kleiman, R.J., Morton, D.O., Neill, S.M., Schmidt, C.J., Weinberg, R.J., Menniti, F.S., 2012. The distribution of phosphodiesterase 2A in the rat brain. Neurosci 226, 145–155. https://doi.org/10.1016/j.neuroscience.2012.09.011.
Steuer Costa, W., Yu, S.-C., Liewald, J.F., Gottschalk, A., 2017. Fast cAMP modulation of neurotransmission via neuropeptide signals and vesicle loading. Curr. Biol. 27, 495–507. https://doi.org/10.1016/j.cub.2016.12.055.
Tabet, R., Moutin, E., Becker, J.A., Heintz, D., Fouillen, L., Flatter, E., Krężel, W., Alunni, V., Koebel, P., Dembélé, D., et al., 2016. Fragile X mental retardation protein (FMRP) control diacylglycerol kinase activity in neurons. Proc. Natl. Acad. Sci. U. S. A. 113, 3619–3628. https://doi.org/10.1073/pnas.1522631113.
Tang, B., Wang, T., Wan, H., Qin, X., Zhang, Y., Wang, J., Yu, C., Berton, F., Francesconi, W., Yates, I.I.I.J.R., et al., 2015. Fmr1 deficiency promotes age-dependent alterations in the cortical synaptic proteome. Proc. Natl. Acad. Sci. U. S. A. 112, 4697–4706. https://doi.org/10.1073/pnas.1502258112.
Thanawala, M., Regehr, W.E., 2013. Presynaptic calcium influx controls neurotransmitter release inpart by regulating the effective size of the readily releasable pool. J. Neurosci. 33, 4625–4633. https://doi.org/10.1523/JNEUROSCI.4031-12.2013.
Till, S.M., Li, H.-L., Miniaci, M.C., Kandel, E.R., Choi, Y.-B., 2011. A presynaptic role fpr

FMRP during protein synthesis-dependent long-term plasticity. Learn. Mem. 18, 39–48. https://doi.org/10.1101/lm.1958811.

Zalfa, F., Dickson, K.S., Mercaldo, V., De Rubeis, S., Di Penta, A., Tabolacci, E., Chiurazzi, P., Neri, G., Grant, S.G., Bagni, C., 2007. A new function for the fragile X mental retardation protein in regulation of PSD-95 mRNA stability. Nat. Neurosci. 10, 578–587. https://doi.org/10.1038/nn1893.

Zhang, C., Yu, Y., Ruan, L., Wang, C., Pan, J., Klabnik, J., Lueptow, L., Zhang, H.T., O'Donnell, J.M., Xu, Y., 2015. The roles of phosphodiesterase 2 in the central nervous and peripheral systems. Curr. Pharm. Des. 21, 274–290. https://doi.org/10.2174/1381612820666140826115245.